Check for updates

Sustainable wastewater treatment by deep eutectic solvents and natural silk for radioactive iodine capture

Li Fu, Xiaohong Hu, Shuyuan Yu, Yarui Guo, He Liu, Wenjing Zhang, Yanyan Lou, Dan Li and Qiqi Yu

ABSTRACT

The pollution from nuclear leaks and nuclear disasters (e.g. radioactive iodine) would cause serious harm to human beings and ecosystems for many years. Cocoon silk and deep eutectic solvents (DESs) are both green substances. DESs are easily synthesized, cheap, highly biocompatible and highly biodegradable. Here, we combine the removal of organic dyes and the capture of radioactive iodine by using green DES-pretreated cocoon silk. It is the first time organic dyes have been removed from wastewater by DES-disrupted silk for the purpose of favourably removing iodine. Organic dyes-captured DES-pretreated cocoon silk could be used to capture iodine efficiently. It opens a new route to dispose of one waste from nuclear energy with organic dyes from wastewater captured by green solvents-pretreated natural silk.

Key words | deep eutectic solvents, green chemistry, green solvents, iodine capture

Li Fu (corresponding author)
Xiaohong Hu
Shuyuan Yu
Yarui Guo
He Liu
Wenjing Zhang
Yanyan Lou
Dan Li
Qiqi Yu
Department of Chemistry and Material Science,
Langfang Normal University,
Langfang 065000, Hebei,
China
E-mail: *2220690@lfnu.edu.cn*

INTRODUCTION

Nuclear energy owns the advantages of low cost, high efficiency and negligible air pollution; however, nuclear disasters (e.g. the Fukushima nuclear explosion) have led to profound harm for human beings. One of the nuclear wastes from nuclear disasters is radioactive iodine (e.g. $^{125/129/131}I_2$) (Sheng *et al.* 2013). For the purpose of better utilizing nuclear energy, it is necessary to design task-specific materials to achieve the fast and reliable capture of iodine. Metal-containing materials would make the efficiency of iodine uptake favorable (Sava *et al.* 2011); however, metal-containing compounds are usually scarce and expensive, impeding large-scale application in real iodine storage. Designing task-specific materials without metal elements (e.g. ionic liquids (ILs) (Wang *et al.* 2014; Yan & Mu 2014; Cao *et al.* 2016; Chen *et al.* 2016; Xue & Xue 2017; Li *et al.* 2018; Wang & Wang 2019)) is cheap; however, ILs are highly volatile (Earle *et al.* 2006), relatively unstable (Wang *et al.* 2017; Xue *et al.* 2018), hygroscopic (Cao *et al.* 2012), synthetically complex and expensive. It is still urgent and challenging to develop new metal-free materials for improved iodine-capturing efficiency.

Deep eutectic solvents (DESs) are the liquid formed by mixing two or more compounds with lower melting points than that of the individual components. It is deemed that the lower melting point of DESs than that of their individual components is attributed to the strong H-bonding interaction between H-bond donor (HBD) and H-bond acceptor (HBA) (Smith *et al.* 2014) or other non-covalent interactions (Yu & Mu 2019; Yu *et al.* 2019). The synthesis of DESs is quite simple compared to other metal-free materials. Most of the raw materials of DESs are natural, inexpensive and biodegradable. Moreover, DESs own the characteristics of negligible toxicity, wide liquid range and high designability (Abbott *et al.* 2004; Paiva *et al.* 2014). Therefore, DESs have been deemed to be green solvents and have been paid much attention in many areas, such as gas capture/conversion, biomass pretreatment/conversion, metal separation, material synthesis and lithium ion batteries (Zhang *et al.* 2012; Boisset *et al.* 2013; Paiva *et al.* 2014; Wang *et al.* 2018a, 2018b; Zhao *et al.* 2018; Mou *et al.* 2019; Tran *et al.* 2019; Zhao *et al.* 2019).

Direct iodine capture by task-specific DESs has been reported. Mu's group for the first time discovered that that DESs absorbed iodine with high efficiency and high recyclability (Li *et al.* 2016). The best DES choline iodide, methylurea (ChI:methylurea, 1:2 mol ratio), could capture iodine with circa 100% removal efficiency within 5 h (Li *et al.* 2016). However, the cost of ChI was still a little high

doi: 10.2166/wst.2019.413

Downloaded from http://iwaponline.com/wst/article-pdf/80/9/1683/764616/wst080091683.pdf
by guest

(ca. 20 RMB per g). The high price of ChI would not be favorable for the industrial application of DESs for widespread iodine capture in practice. Cheap DESs containing PEG were thus developed for radioactive iodine capture. Chen *et al.* found that DES PEG200:thiourea (2:1) showed the best absorption performance on iodine capture among all the pure PEG-based DESs (Chen *et al.* 2019a). Although PEG in DESs was cheap and green, thiourea in DESs was deemed as carcinogenic in the List of IARC Group 3. The above improvements had presented an interesting idea of iodine capture. The simultaneous achievement of high efficiency, low cost and high sustainability is challenging. Therefore, there is still room for the improvement of direct capture of iodine.

Organic dyes are organic compounds with a certain color, which are used in a wide range of applications such as clothing and food. Although organic dyes add color to our lives, they also lead to pollution to our environment (e.g. water pollution), which further damages human health and the ecosystem. How to develop cheap and green material or process to capture organic dyes (e.g. methylene blue, Rhodamine B, Coomassie Brilliant Blue) from wastewater efficiently is still challenging and interesting. Here, we develop a new strategy to capture iodine by absorption and radioactive capture of a couple of organic dyes. The organic dye is first adsorbed by a DES-pretreated silk, which has the advantages of simple operation, short time consumption and low cost. Then, iodine could be captured by the pretreated silk@dyes core shell material. The aim of our work is to develop a new strategy for disposing of one waste (i.e. radioactive iodine) from nuclear energy with another waste from polluted water (i.e. organic dyes) by utilizing green solvents and natural silk. It is the first time that the process of two wastes in sequence has been combined via sustainable solvents, to the best of our knowledge.

EXPERIMENTAL SECTION

Materials

Urea (≥99.0%), guanidine hydrochloride (98.0%) and iodine (≥99.8) were purchased from Sinopharm Chemical Reagent Co., Ltd. The organic dyes (Brilliant Blue G, Rhodamine B, methylene blue, Figure 1) were purchased from Macklin. Cyclohexane (99.5%) was purchased from Fuchen Chemical Reagents Co., Ltd. Sodium carbonate (Na_2CO_3, AR) was purchased from Tianjin North Tianyi Chemical Reagent Co., Ltd.

DES synthesis

DES was synthesized by mixing and stirring two components (i.e. urea and guanidine hydrochloride with the molar ratio of 2:1, Figure 1) at 80 °C until a clear liquid appeared (Tan *et al.* 2018). No impurities were detected in the DES via the techniques of nuclear magnetic resonance (NMR) and Fourier transform infrared (FT-IR) spectroscopy.

Cocoon silk pretreatment

The method of silk pretreatment (Figure 2) was similar to that of Mu's report (Tan *et al.* 2018). First, 0.047 M Na_2CO_3 water solution was used to degum natural silk at 100 °C for 30 minutes twice. After being dried in an oven

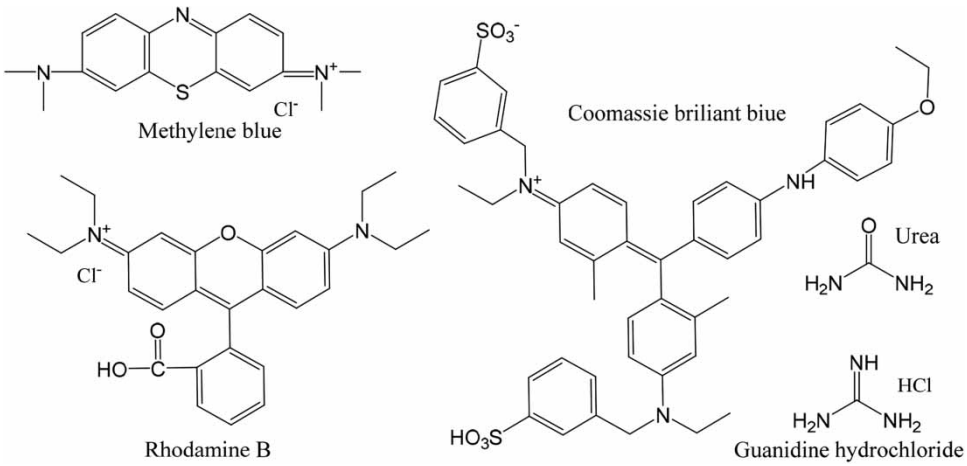

Figure 1 | Chemical structure of organic dyes and components of DES.

Downloaded from http://iwaponline.com/wst/article-pdf/80/9/1683/764616/wst080091683.pdf
by guest

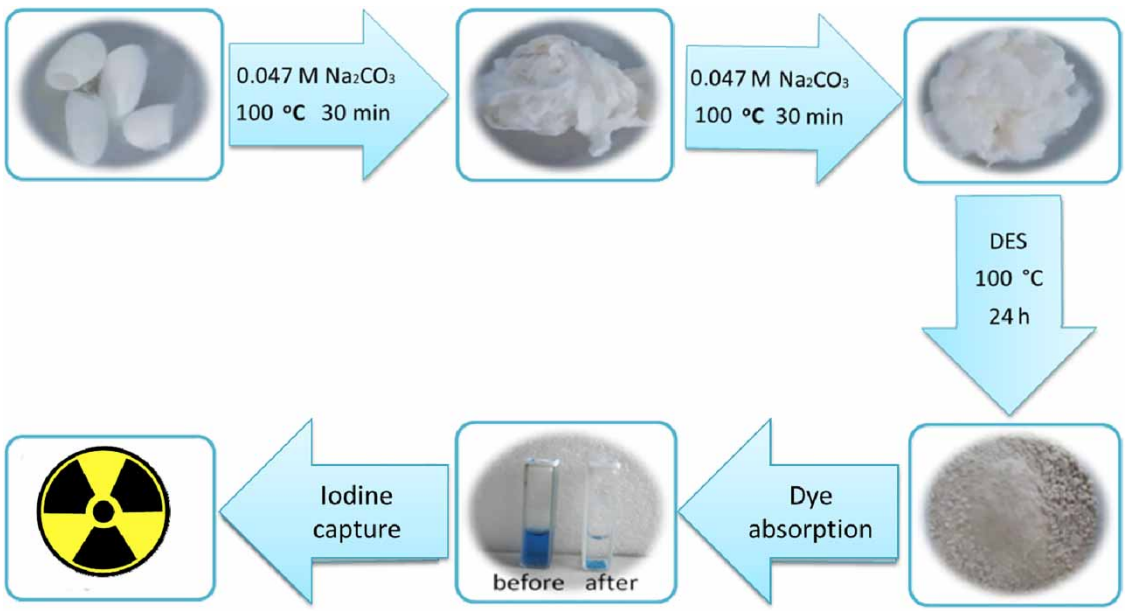

Figure 2 | The process of utilizing natural silk: degumming, dissolution, dye adsorption and regeneration.

at 60 °C for 24 h, the degummed silk was pretreated in DES media (1:50 wt/wt silk/DES) at 100 °C for 24 hours. The final product was obtained by being sonicated in deionized water (1:500 wt/wt silk/water) for 4 h, then centrifuged and dried in an oven at 60 °C for 24 h.

Dye absorption

First, a certain amount of pretreated cocoon silk was put at the bottom of the quartz cell. Then, 2 mL dye water solution with a certain concentration was added into the quartz cell. The absorbance was recorded as a function of time by using a spectrophotometer (722G, 588 nm for Brilliant Blue G, 554 nm for Rhodamine B, 662 nm for methylene blue).

IR spectra

All the IR spectra were measured by FT-IR instrument (IR Prestige-21, Shimadzu). Parameters of FT-IR were: 4 cm^{-1} resolution, 40 scans, and 400–4,000 cm^{-1} range. Specifically, dry KBr pellet was recorded first as the background. Then, pellets of samples/KBr homogeneous mixtures were used for IR measurement.

Iodine capture

The method of iodine capture was similar to that of Mu's work (Yan & Mu 2014). First, iodine absorbent (0.035 g) was placed in the bottom of the quartz cell. Then, 2 mL iodine cyclohexane solution (0.4 g L^{-1}) was added into the quartz cell above. The absorbance was recorded as a function of time by using the spectrophotometer (722G, 522 nm (Yan & Mu 2014) for iodine cyclohexane solution).

RESULTS AND DISCUSSION

Organic dye capture

Figure 3 shows the effect of mass (0.005 g, 0.01 g, 0.02 g, 0.03 g) on the absorption of organic dyes by disrupted silk. Rhodamine B was selected as the representative organic dyes. The concentration and volume of rhodamine B water solution were fixed at 10 μM and 2 mL, respectively. The vertical axes of Figure 3(a) and 3(b) show the removal efficiency with the unit of % and % μg^{-1}, respectively.

Figure 3(a) displays a little difference in the rhodamine B removal efficiency among different masses of disrupted silk. The capture efficiency of 0.02 and 0.03 g pretreated silk is almost the same. The removal efficiency of rhodamine B by 0.005 g pretreated silk is only a little lower. The similar removal efficiency might be related to the similar surface area of the four pretreated silk samples on the bottom of the quartz cell.

In this way, if % μg^{-1} is used as the vertical axis, the difference in removal efficiency affected by the mass of

Downloaded from http://iwaponline.com/wst/article-pdf/80/9/1683/764616/wst080091683.pdf
by guest

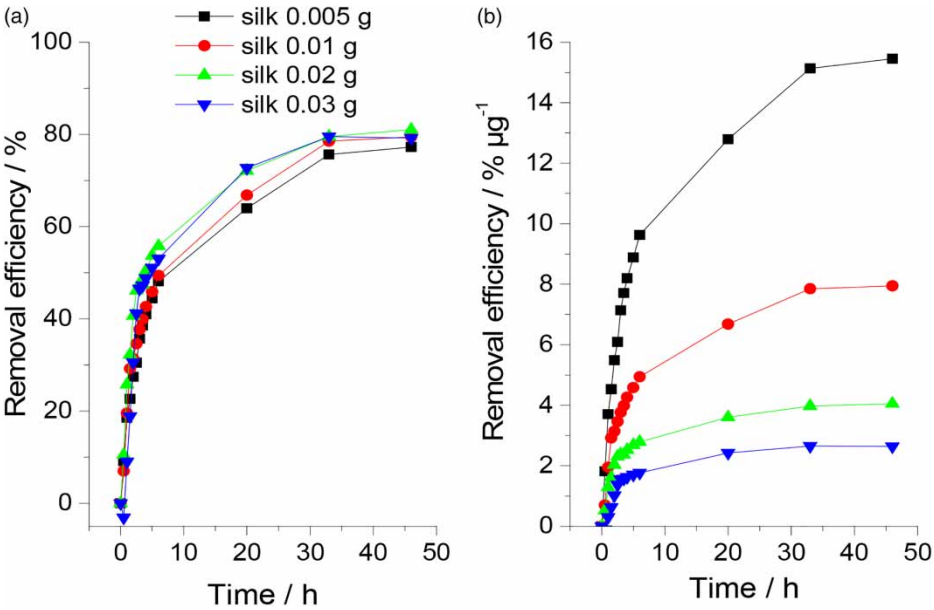

Figure 3 | Effect of the weight of disrupted silk on Rhodamine B (10 μM, 2 mL) adsorption with the removal efficiency expressed by % (a) and % μg^{-1} (b).

pretreated silk is obvious (Figure 3(b)). Specifically, the order of removal efficiency is listed as: 0.005 g > 0.01 g > 0.02 g > 0.03 g. This means that lower mass of pretreated silk would obtain higher removal efficiency when using % μg^{-1} as the unit. However, in a real application, both the units (% and % μg^{-1}) should be considered. This is because the former represents the absolute efficiency and the latter represents the relative efficiency.

The effect of various organic dyes from a fixed mass of pretreated silk (0.01 g) is also investigated (Figure 4). Methylene blue, Rhodamine B and Coomassie Brilliant Blue are selected as the representative organic dyes. The above three organic dyes are common dyes for industrial application. For the purpose of a better comparison, all the concentrations and volumes of organic dyes are fixed at 10 μM and 2 mL, respectively.

A noticeable result for the effect of organic dyes is that choosing the unit of % (Figure 4(a)) or % μg^{-1} (Figure 4(b)) has no effect on the comparison of dye removal efficiency. The tendency of Figure 4(a) and 4(b) is the same. This is because the mass of three organic dyes is the same and that % μg^{-1} is derived from the removal efficiency (%) divided by the mass (μg).

From Figure 4 we can conclude that the removal efficiency of organic dyes by pretreated silk is ordered as: methylene blue > Rhodamine B > Coomassie Brilliant Blue. In contrast with the pristine silk, the pretreated silk owns a higher rate of methylene blue absorption but a comparable capacity in the same condition. This might be attributed to the higher exposure of functionalized groups for the DES-pretreated cocoon silk than the pristine silk (Tan *et al.* 2018).

Owing to the highest removal efficiency of methylene blue, we selected methylene blue to study the concentration factor. The effect of dye concentration on dye absorption by pretreated silk is shown in Figure 5. Four concentrations of methylene blue (10 μM, 20 μM, 40 μM, 80 μM) are selected. The mass of pretreated silk is also 0.01 g for all the measurements. The result shows that it is faster to remove methylene blue when the dye concentration is lower (Figure 5). However, for all four concentrations, their differences in removal capacity are very little.

Apart from the absorbance data by spectrophotometer, the organic dye's removal could be directly visualized. Photos of dye color (methylene blue, 10 μM, 2 mL) by pretreated silk (0.01 g) as a function of time are shown in Figure 6. The result shows that the blue color of methylene blue turns to light blue and then to nearly transparent at 46 h.

To further corroborate the methylene blue absorption from water solution by pretreated silk, IR spectra were conducted (Figure 7(a)). In the wavenumber range less than 2,400 cm^{-1}, three IR bands around 2,357 cm^{-1}, 1,605 cm^{-1} and 1,342 cm^{-1} of methylene blue disappeared after being captured by pretreated silk. This suggests that there is strong interaction between methylene blue and pretreated silk. Moreover, the band range from 3,000 cm^{-1}

Downloaded from http://iwaponline.com/wst/article-pdf/80/9/1683/764616/wst080091683.pdf
by guest

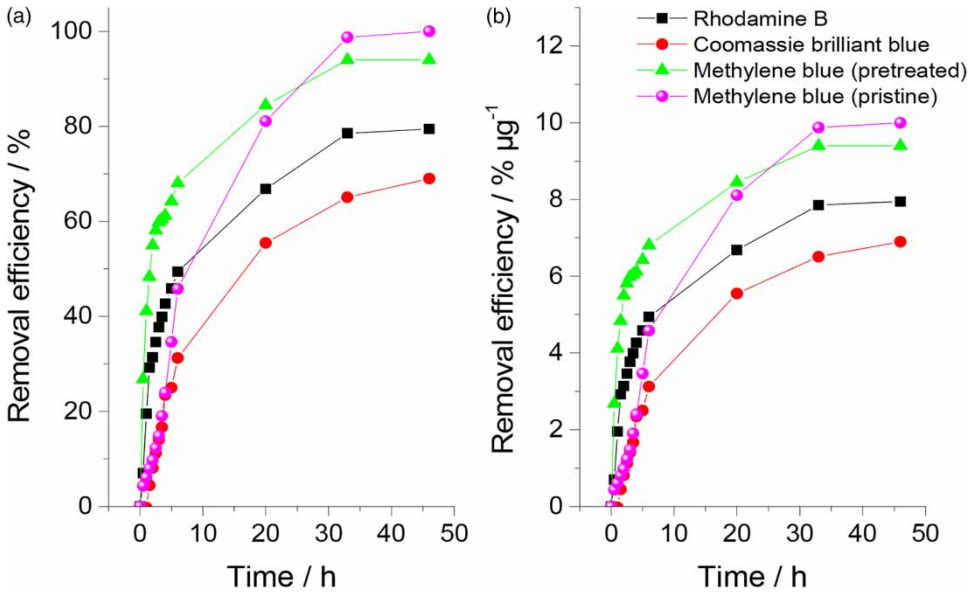

Figure 4 | Different dyes' absorption (10 μM, 2 mL) by disrupted silk (0.01 g) with the removal efficiency expressed by % (a) and % μg^{-1} (b).

to 2,000 cm^{-1} is broadened and heightened for dye-absorbed silk when compared to pure dye and pure silk. It also provides the evidence of strong interaction between methylene blue and pretreated cocoon silk.

The mechanism of absorption of dyes by pretreated silk can be suggested as below by selecting methylene blue as the representative organic dye (Figure 7(b)). After pretreatment by DES, natural silk would expose more active sites such as C = O, NH. The exposed C = O is able to interact with the cation N in methylene blue. Meanwhile, NH in pretreated silk would form strong H-bonds with S and N in methylene blue. Because there are different compounds in pretreated silk, such as Gly-Gly, Gly-Ala, Gly-Ser, many categories of functional sites would exist in pretreated silk to form H-bonds with N and S in methylene blue. Therefore, a broad added peak appears in pretreated silk after the absorption of methylene blue, as shown in Figure 7(b).

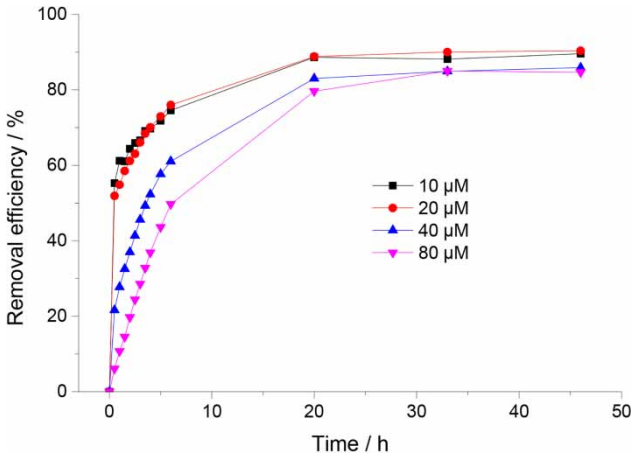

Figure 5 | Relationship between removal efficiency of methylene blue by disrupted silk (0.01 g) and dye concentration (2 mL) with the removal efficiency expressed by %.

Iodine capture

Figure 8 shows the iodine capture by methylene blue-absorbed DES-pretreated cocoon silk. Methylene blue is selected as the representative organic dye because of its having the highest absorption capacity by DES-pretreated cocoon silk. The mass of iodine absorbent is fixed at 0.035 g. The volume and concentration of iodine cyclohexane solution is 2 mL and 0.4 g L^{-1}, respectively.

The result shows that pure methylene blue owns the highest iodine capture capacity among all the three iodine absorbents. The removal efficiency of iodine by methylene blue reaches ca. 90% within 11 h. It gives us a hint that the decoration of methylene blue on the surface of pretreated cocoon silk would improve the efficiency of iodine capture. As expected, we find in Figure 8 that pure pretreated cocoon silk captures iodine with a lower efficiency than methylene blue-absorbed DES-pretreated cocoon silk.

We attribute the higher iodine removal efficiency by methylene blue pretreated silk than by pretreated silk to the presence of methylene blue. Compared to the previously reported iodine capture by DESs (Li *et al.* 2016;

Downloaded from http://iwaponline.com/wst/article-pdf/80/9/1683/764616/wst080091683.pdf
by guest

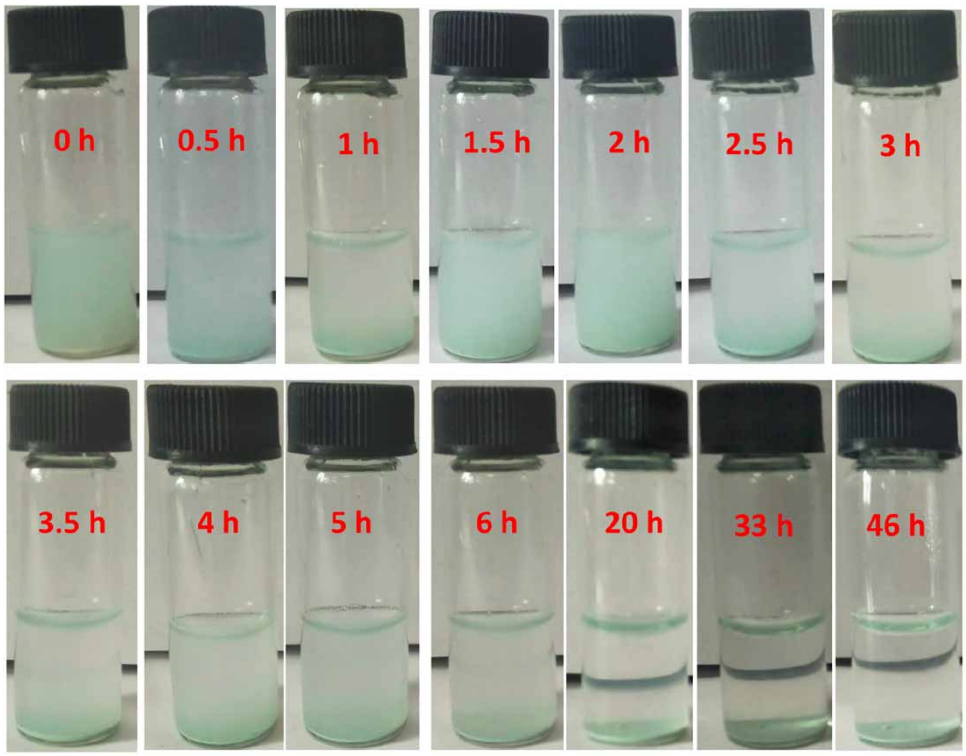

Figure 6 | Color change of methylene blue (10 μM, 2 mL) as a function of time by 0.01 g disrupted silk.

Chen *et al.* 2019a), the rate and capacity of iodine capture by methylene blue pretreated silk is a little lower. However, our work combines the organic dye absorption and iodine capture related to green solvents and green cocoon silk for the first time. It also provides a new strategy to use one waste to dispose of another waste with green solvents.

Comparison of iodine capture

Radioactive iodine capture by methylene blue-pretreated silk in our work is compared to previous reported research. Mu *et al.* reported that ChI:thiourea owned the highest iodine-removing efficiency, i.e. circa 100% removal efficiency after 5 h (Li *et al.* 2016). Chen *et al.* reported that removal efficiency of the best DES PEG200:thiourea could be as high as 100% within 3 h (Chen *et al.* 2019a). Here, we report that methylene blue could capture circa 90% of the iodine within 11 h. The iodine removal efficiency by methylene blue-pretreated silk is circa 30% within 11 h, which is lower than the previous reports. However, compared to previous reports, our methods are greener and more sustainable. More important, we aim to make full use of disposing of one waste (wastewater) to act as the absorbent to sustainably treat another waster (radioactive iodine).

Kinetics

We also use the equation $E = E_{\infty}(1 - e^{-kt})$ to fit the iodine capture by methylene blue, pretreated silk, and methylene blue-absorbed pretreated silk as a function of time (Figure 8 and Table 1). This equation is similar to the water absorption fitting by ILs and DESs, as reported by Mu's group (Chen *et al.* 2019b). In this equation, E and E_{∞} mean the iodine removal efficiency at some time point and at the steady state with the unit of %, respectively. Parameters k and t indicate the fitted value (h^{-1}) and time (h), respectively. 1/k and kE_{∞} represent the difficulty of reaching equilibrium and the average iodine capture rate, respectively (Chen *et al.* 2019b). Three parameters, $R_{1\,h}$, $R_{1\,h,cal}$, kE_{∞}, are all indicative of iodine capture rate (measured initial rate, calculated initial rate, average rate).

Figure 8 shows that the fitted curve is favorable for the iodine capture by methylene blue, pretreated silk, and methylene blue-absorbed pretreated silk. It could also be corroborated by the value of R^2 in Table 1, which is close to 1. The lowest and highest value of R^2 is 0.959 and

Downloaded from http://iwaponline.com/wst/article-pdf/80/9/1683/764616/wst080091683.pdf
by guest

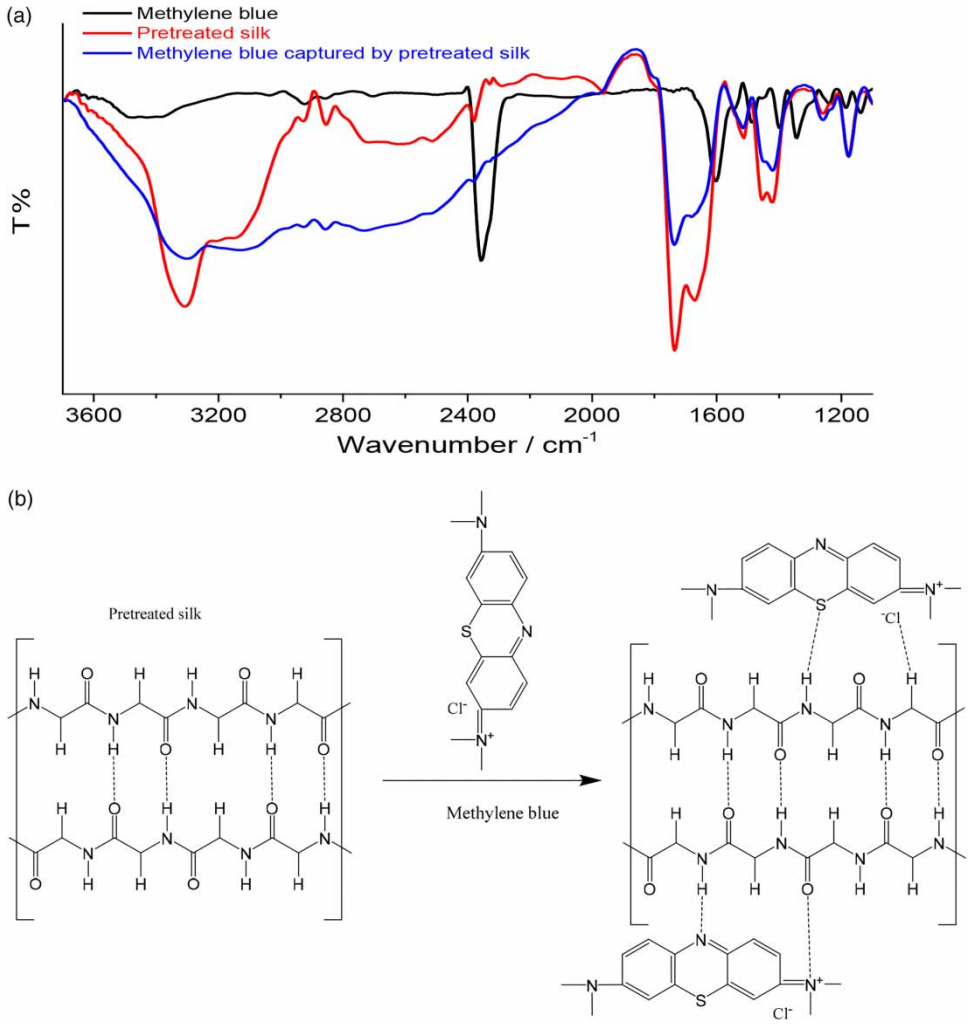

Figure 7 | FT-IR transmittance spectra of methylene blue, DES-pretreated cocoon silk and methylene blue (2 mL, 10 μM) capture by DES-pretreated cocoon silk (0.01 g, 46 h) (a). Proposed absorption mechanism of methylene blue by pretreated cocoon silk (b).

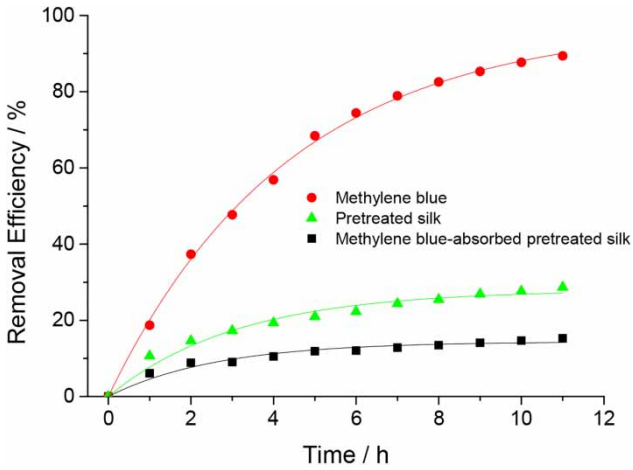

Figure 8 | Iodine capture by methylene blue, pretreated silk, and methylene blue-absorbed pretreated silk as a function of time. The mass of absorbent is fixed at 0.035 g. The volume and concentration of iodine cyclohexane solution is 2 mL and 0.4 g L^{-1}, respectively. The lines are the fitted lines.

0.998, respectively. The calculated initial rate within 1 h ($R_{1\,h,cal}$) is slightly different from the measured initial rate within 1 h ($R_{1\,h}$). Although there is some difference between $R_{1\,h,cal}$ and $R_{1\,h}$, the fitted equation $E = E_\infty(1 - e^{-kt})$ still well describes the kinetics of iodine capture by the investigated absorbents. Moreover, in terms of the average rate (kE_∞), this value is also slightly different from the above two initial rates.

Comparison of three iodine-capturing absorbents (Table 1) shows that the iodine capture rate order is: methylene blue > methylene blue-absorbed pretreated silk > pretreated silk. Specifically, the order is the same both for the initial rate and the average rate. The order of iodine capture capacity ($E_{11\,h}$ and E_∞) is the same as the order of iodine capture rate above: methylene blue > methylene blue-absorbed pretreated silk > pretreated silk.

Downloaded from http://iwaponline.com/wst/article-pdf/80/9/1683/764616/wst080091683.pdf
by guest

Table 1 | Fitted parameters of iodine capture by methylene blue, pretreated silk, and methylene blue-absorbed pretreated silk with the equation $E = E_{\infty}(1 - e^{-kt})$

Iodine absorbents	Capacity $E_{11\,h}$/%	E_{∞}/%	Rate $R_{1\,h}$/% h^{-1}	$R_{1\,h,cal}$/% h^{-1}	kE_{∞}/% h^{-1}	Equilibrium 1/k/h	R^2
Methylene blue	89.4	97.9 ± 1.34	18.7	20.1	22.5 ± 0.01	4.4 ± 0.01	0.998
Methylene blue-absorbed pretreated silk	28.7	28 ± 1.03	10.6	7.7	9.0 ± 0.04	3.1 ± 0.04	0.972
Pretreated silk	15.3	14.4 ± 0.54	6.1	4.5	5.5 ± 0.03	2.6 ± 0.05	0.959

Similarly, the difficulty in reaching equilibrium for iodine capture also owns the same order: methylene blue > methylene blue-absorbed pretreated silk > pretreated silk.

The above results suggest that methylene blue-absorbed pretreated silk owns the middle iodine capture capacity, rate and equilibrium when compared to pure methylene blue and pure pretreated silk. Specifically, both the capacity and rate of methylene blue-absorbed pretreated silk is two times that of pure pretreated silk (Figure 8 and Table 1). This could be ascribed to the increased effect of methylene blue for iodine capture.

CONCLUSION

In summary, we for the first time develop a strategy for utilizing a green and sustainable way to treat wastewater and remove radioactive iodine by green DESs and natural silk. Both DESs and natural silk are easily available, very cheap, highly biocompatible and highly biodegradable. The removal efficiency of organic dyes by pretreated silk is ordered as: methylene blue > Rhodamine B > Coomassie Brilliant Blue. The order of removal efficiency influenced by mass of disrupted silk is listed as: 0.005 g > 0.01 g > 0.02 g > 0.03 g. In contrast with the pristine silk, the pretreated silk owns a higher rate of methylene blue absorption but a comparable capacity in the same condition. It is quicker to remove methylene blue when the dye concentration is lower. Comparison of three iodine-capturing absorbents shows that the iodine capture rate order is: methylene blue > methylene blue-absorbed pretreated silk > pretreated silk. More importantly, organic dye-captured DES-pretreated cocoon silk shows favorable iodine capture efficiency, which is two times that of pure pretreated silk. The detailed mechanism is expected to be investigated in detail in our group.

NOTES

The authors declare no competing financial interests.

ACKNOWLEDGEMENTS

This work was supported by the Natural Science Foundation of Hebei Province with Grant number B2016408027.

REFERENCES

Abbott, A. P., Boothby, D., Capper, G., Davies, D. L. & Rasheed, R. K. 2004 Deep eutectic solvents formed between choline chloride and carboxylic acids: versatile alternatives to ionic liquids. *Journal of the American Chemical Society* **126** (29), 9142–9147.

Boisset, A., Menne, S., Jacquemin, J., Balducci, A. & Anouti, M. 2013 Deep eutectic solvents based on N-methylacetamide and a lithium salt as suitable electrolytes for lithium-ion batteries. *Physical Chemistry Chemical Physics* **15** (46), 20054–20063.

Cao, Y. Y., Chen, Y., Sun, X. F., Zhang, Z. M. & Mu, T. C. 2012 Water sorption in ionic liquids: kinetics, mechanisms and hydrophilicity. *Physical Chemistry Chemical Physics* **14** (35), 12252–12262.

Cao, B., Liu, S., Du, D., Xue, Z., Fu, H. & Sun, H. 2016 Experiment and DFT studies on radioiodine removal and storage mechanism by imidazolium-based ionic liquid. *Journal of Molecular Graphics and Modelling* **64**, 51–59.

Chen, Y., Zhang, F. G. & Xue, Z. M. 2016 Iodine capture by ionic liquids and recovery by compressed CO_2. *Journal of Molecular Liquids* **223**, 202–208.

Chen, Y., Li, G., Yu, S., Guo, Z., Dong, Z. & Wang, S. 2019a Efficient iodine capture by biocompatible PEG-based deep eutectic solvents: kinetics and dynamic mechanism. *Journal of Molecular Liquids* **289**, 111166.

Chen, Y., Yu, D., Chen, W., Fu, L. & Mu, T. 2019b Water absorption by deep eutectic solvents. *Physical Chemistry Chemical Physics* **21** (5), 2601–2610.

Earle, M. J., Esperanca, J., Gilea, M. A., Lopes, J. N. C., Rebelo, L. P. N., Magee, J. W., Seddon, K. R. & Widegren, J. A. 2006 The distillation and volatility of ionic liquids. *Nature* **439** (7078), 831–834.

Li, G., Yan, C., Cao, B., Jiang, J., Zhao, W., Wang, J. & Mu, T. 2016 Highly efficient I_2 capture by simple and low-cost deep eutectic solvents. *Green Chemistry* **18** (8), 2522–2527.

Li, R., Zhao, Y., Chen, Y., Liu, Z., Han, B., Li, Z. & Wang, J. 2018 Imidazolate ionic liquids for high-capacity capture and reliable storage of iodine. *Communications Chemistry* **1**, 69.

Downloaded from http://iwaponline.com/wst/article-pdf/80/9/1683/764616/wst080091683.pdf
by guest

List of IARC Group 3 possible carcinogens Available from: https://en.wikipedia.org/wiki/List_of_IARC_Group_3_carcinogens (accessed June 2019).

Mou, H., Wang, J., Zhang, D., Yu, D., Chen, W., Wang, D. & Mu, T. 2019 A one-step deep eutectic solvent assisted synthesis of carbon nitride/metal oxide composites for photocatalytic nitrogen fixation. *Journal of Materials Chemistry A* **7** (10), 5719–5725.

Paiva, A., Craveiro, R., Aroso, I., Martins, M., Reis, R. L. & Duarte, A. R. C. 2014 Natural deep eutectic solvents – solvents for the 21st century. *ACS Sustainable Chemistry & Engineering* **2** (5), 1063–1071.

Sava, D. F., Rodriguez, M. A., Chapman, K. W., Chupas, P. J., Greathouse, J. A., Crozier, P. S. & Nenoff, T. M. 2011 Capture of volatile iodine, a gaseous fission product, by zeolitic imidazolate framework-8. *Journal of the American Chemical Society* **133** (32), 12398–12401.

Sheng, X., Freeman, S. P. H. T., Xiaolin, H., Akira, W., Katsuhiko, Y. & Luyuan, Z. 2013 Iodine isotopes in precipitation: temporal responses to ^{129}I emissions from the Fukushima nuclear accident. *Environmental Science & Technology* **47** (19), 10851–10859.

Smith, E. L., Abbott, A. P. & Ryder, K. S. 2014 Deep eutectic solvents (DESs) and their applications. *Chemical Reviews* **114** (21), 11060–11082.

Tan, X. X., Zhao, W. C. & Mu, T. C. 2018 Controllable exfoliation of natural silk fibers into nanofibrils by protein denaturant deep eutectic solvent: nanofibrous strategy for multifunctional membranes. *Green Chemistry* **20** (15), 3625–3633.

Tran, M. K., Rodrigues, M.-T. F., Kato, K., Babu, G. & Ajayan, P. M. 2019 Deep eutectic solvents for cathode recycling of Li-ion batteries. *Nature Energy* **4** (4), 339–345.

Wang, X. & Wang, Z. 2019 Enhanced iodine uptake in ionic liquid by biomass, solvents, or supported materials. *International Journal of Environmental Science and Technology* **16** (7), 3317–3324.

Wang, Y. H., Tong, J. Y., Wu, W. H. & Lu, Y. X. 2014 Halogen bonds between I_2 and ion pairs: interpreting the ability of ionic liquids in efficient capture of radioactive iodine. *Computational and Theoretical Chemistry* **1049**, 97–101.

Wang, B., Qin, L., Mu, T., Xue, Z. & Gao, G. 2017 Are ionic liquids chemically stable? *Chemical Reviews* **117** (10), 7113–7131.

Wang, J., Mou, H., Li, R., Li, Y., Wang, D., Xue, Z. & Mu, T. 2018a Solution processing of V_2VI_3 chalcogenides with a deep eutectic solvent for enhanced visible-light-driven hydrogen production. *Green Chemistry* **20** (23), 5266–5270.

Wang, J., Wang, P., Wang, Q., Mou, H., Cao, B., Yu, D., Wang, D., Zhang, S. & Mu, T. 2018b Low temperature electrochemical deposition of aluminum in organic bases/thiourea-based deep eutectic solvents. *ACS Sustainable Chemistry & Engineering* **6** (11), 15480–15486.

Xue, Z. & Xue, Z. 2017 The high-efficiency and eco-friendly PEGylated ionic liquid systems for radioactive iodine capture through halogen bonding interaction. *Journal of Molecular Liquids* 238, 106–114.

Xue, Z., Qin, L., Jiang, J., Mu, T. & Gao, G. 2018 Thermal, electrochemical and radiolytic stabilities of ionic liquids. *Physical Chemistry Chemical Physics* **20** (13), 8382–8402.

Yan, C. Y. & Mu, T. C. 2014 Investigation of ionic liquids for efficient removal and reliable storage of radioactive iodine: a halogen-bonding case. *Physical Chemistry Chemical Physics* **16** (11), 5071–5075.

Yu, D. & Mu, T. 2019 Strategy to form eutectic molecular liquids based on noncovalent interactions. *The Journal of Physical Chemistry B* **123** (23), 4958–4966.

Yu, D., Mou, H., Zhao, X., Wang, Y. & Mu, T. 2019 Eutectic molecular liquids based on hydrogen bonding and π-π interaction for exfoliating two-dimensional materials and recycling polymers. *Chemistry – An Asian Journal* **14** (19), 3350–3356.

Zhang, Q., Vigier, K. D. O., Royer, S. & Jerome, F. 2012 Deep eutectic solvents: syntheses, properties and applications. *Chemical Society Reviews* **41** (21), 7108–7146.

Zhao, X., Lan, X., Yu, D., Fu, H., Liu, Z. & Mu, T. 2018 Deep eutectic-solvothermal synthesis of nanostructured Fe_3S_4 for electrochemical N_2 fixation under ambient conditions. *Chemical Communications* **54** (92), 13010–13013.

Zhao, J., Zhang, J., Yang, W., Chen, B., Zhao, Z., Qiu, H., Dong, S., Zhou, X., Cui, G. & Chen, L. 2019 'Water-in-deep eutectic solvent' electrolytes enable zinc metal anodes for rechargeable aqueous batteries. *Nano Energy* **57**, 625–634.

First received 4 October 2019; accepted in revised form 6 December 2019. Available online 19 December 2019

Downloaded from http://iwaponline.com/wst/article-pdf/80/9/1683/764616/wst080091683.pdf
by guest